Published OnlineFirst April 20, 2011; DOI: 10.1158/0008-5472.CAN-10-3816

Identification of Aldo-Keto Reductase AKR1B10 as a Selective Target for Modification and Inhibition by Prostaglandin A_1: Implications for Antitumoral Activity

Beatriz Díez-Dacal[1], Javier Gayarre[1], Severine Gharbi[3], John F. Timms[3], Claire Coderch[2], Federico Gago[2], and Dolores Pérez-Sala[1]

Abstract

Cyclopentenone prostaglandins (cyPG) are reactive eicosanoids that may display anti-inflammatory and antiproliferative actions, possibly offering therapeutic potential. Here we report the identification of members of the aldo-keto reductase (AKR) family as selective targets of the cyPG prostaglandin A_1 (PGA_1). AKR enzymes metabolize aldehydes and drugs containing carbonyl groups and are involved in inflammation and tumorigenesis. Thus, these enzymes represent a class of targets to develop small molecule inhibitors with therapeutic activity. Molecular modeling studies pointed to the covalent binding of PGA_1 to Cys299, close to the active site of AKR, with His111 and Tyr49, which are highly conserved in the AKR family, playing a role in PGA_1 orientation. Among AKR enzymes, AKR1B10 is considered as a tumor marker and contributes to tumor development and chemoresistance. We validated the direct modification of AKR1B10 by biotinylated PGA_1 (PGA_1-B) in cells, and confirmed that mutation of Cys299 abolishes PGA_1-B incorporation, whereas substitution of His111 or Tyr49 reduced the interaction. Modification of AKR1B10 by PGA_1 correlated with loss of enzymatic activity and both effects were increased by depletion of cellular glutathione. Moreover, in lung cancer cells PGA_1 reduced tumorigenic potential and increased accumulation of the AKR substrate doxorubicin, potentiating cell-cycle arrest induced by this chemotherapeutic agent. Our findings define PGA_1 as a new AKR inhibitor and they offer a framework to develop compounds that could counteract cancer chemoresistance. *Cancer Res; 71(12); 4161–71.* ©*2011 AACR.*

Introduction

Cyclopentenone prostaglandins (cyPG) are endogenous reactive eicosanoids which display varied biological actions including inhibition of proinflammatory gene expression and modulation of cell proliferation and redox status (1–3). cyPG arise from the spontaneous dehydration of various PG or from nonenzymatic peroxidation of arachidonic acid. These eicosanoids possess an α,β-unsaturated carbonyl group in the cyclopentene ring which confers them a high reactivity toward nucleophiles, such as thiol groups, and can lead to the formation of covalent adducts by Michael addition. This property is essential for cyPG biological actions (4), including PPAR activation (5) and inhibition of NF-κB and AP-1 transcription factors (1, 6). A- and J-series cyPG were initially observed to share several protein targets and biological actions (7–9). However, recent studies have shown that cyPG with different structures may target selective subsets of cellular proteins (10), and even different residues within the same protein. Ras proteins and histone deacetylases constitute examples of this intra- and intermolecular selectivity (9, 11). Identification of the factors involved in the selectivity of protein modification by different cyPG, as well as of the selectively modified targets, could unveil potential opportunities for drug discovery.

Using proteomic approaches we have identified proteins of the aldo-keto reductase (AKR) family as targets for selective modification by PGA_1 compared with 15-deoxy-$\Delta^{12,14}$-prostaglandin J_2 (15d-PGJ_2). AKR enzymes are involved in the metabolism of several ketones and aldehydes and play important roles in pathophysiology (12). Among them, AKR1B10 exerts key roles in tumor biology. AKR1B10, first identified in human hepatocarcinoma (13), is overexpressed in colorectal, breast and lung cancer, for which it is considered a diagnostic marker (14, 15), and may play a pathogenic role in hepatocellular carcinoma (16) and in tobacco-related carcinogenesis (14, 17). Proposed AKR1B10-mediated tumorigenic mechanisms include retinoic acid depletion and cancer cell dedifferentiation (18, 19) as well as chemoresistance due to metabolism of carbonyl group–bearing anticancer drugs

Authors' Affiliations: [1]Department of Chemical and Physical Biology, Centro de Investigaciones Biológicas, CSIC; [2]Universidad de Alcalá de Henares, Madrid, Spain; and [3]Cancer Proteomics Laboratory, EGA Institute for Women's Health, University College London, London, United Kingdom

Note: Supplementary data for this article are available at Cancer Research Online (http://cancerres.aacrjournals.org/).

Corresponding Author: Dolores Pérez-Sala, Department of Chemical and Physical Biology, Centro de Investigaciones Biológicas, CSIC, Ramiro de Maeztu, 9, 28040 Madrid, Spain. Phone: 34-918373112; Fax: 34-915360432; E-mail: dperezsala@cib.csic.es

doi: 10.1158/0008-5472.CAN-10-3816

Published OnlineFirst April 20, 2011; DOI: 10.1158/0008-5472.CAN-10-3816

(20). Therefore, AKR1B10 constitutes a primary target for the development of inhibitors with anticancer potential.

Here we have confirmed the direct modification of AKR1B10 by PGA_1-B and show that this cyPG inhibits AKR activity. Moreover, PGA_1 treatment potentiated the effects of the carbonyl group–containing drug doxorubicin. These results provide a novel approach for the inhibition of AKR1B10 which could be exploited in the design of strategies to overcome cancer chemoresistance.

Materials and Methods

Reagents

Prostanoids and their biotinylated analogues [15d-PGJ_2-biotin (15d-PGJ_2-B) and prostaglandin A_1-biotin (PGA_1-B)] were from Cayman Chemical. Horseradish peroxidase (HRP)–streptavidin and enhanced chemiluminescence (ECL) reagents were from GE Biosciences. Neutravidin-agarose was from Pierce. Anti-aldose reductase (sc-33219) and anti-GAPDH (sc-32233) were from Santa Cruz Biotechnology and anti-AKR1B10 from Origene.

Cell culture and treatments

NIH-3T3, H1299, and COS-7 cells were from ATCC. A549 and Calu-3 cells were gifts of Dr. F. Rodríguez-Pascual (21, 22) and Dr. A. Silva, respectively. All cells were used within 6 months after resuscitation. NIH-3T3 and COS-7 cells were cultured in Dulbecco's modified Eagle's medium (Invitrogen) containing 10% FBS, 2 mmol/L glutamine, 100 U/mL penicillin, and 100 μg/mL streptomycin. A549 cells were grown in RPMI1640 with the above supplements plus 50 μg/mL gentamycin. For treatments, cells at a confluence of 80% to 90% (COS-7) or 60% to 70% (A549) were incubated in serum-free medium, unless otherwise stated. Cell fractionation into S100 and P100 fractions was done as described (23).

Protein identification

S100 fractions from control or PGA_1-B–treated NIH-3T3 cells were purified on neutravidin beads and analyzed by liquid chromatography/tandem mass spectrometry (LC/MS-MS; ref. 23). Total cell lysates (100 μg of total protein) from control, and 15d-PGJ_2-B– or PGA_1-B–treated NIH-3T3 fibroblasts were analyzed by 2D-electrophoresis as described (24). Gels run in duplicate were either transferred to Immobilon-P membranes to specifically detect proteins which had incorporated the biotinylated PG with HRP–streptavidin and ECL or stained with colloidal Coomassie blue. Gel images were aligned and spots of interest were excised and proteolyzed with trypsin as detailed previously (23, 25). Digests (0.5 μL) were spotted onto a MALDI target in 1 μL of matrix (2,5-dihydroxybenzoic acid). Matrix-assisted laser desorption/ionization–time-of-flight mass spectrometry (MALDI-TOF MS) was carried out on a calibrated Ultraflex time-of-flight mass spectrometer in reflectron mode (Bruker Daltonik). All mass spectra were internally calibrated with trypsin autolysis peaks at m/z 842.51 and m/z 2,211.10. Peptide masses were searched against the IPI Human database using MASCOT version 2.0.02 (Matrix Sciences). Identifications were accepted when a minimum of 6 peptide masses matched a particular protein (mass error of ± 50 ppm allowing 1 missed cleavage), sequence coverage was more than 30%, MOWSE scores were higher than the threshold value ($P = 0.05$), and the predicted protein mass agreed with the gel-based mass.

Molecular modeling

The 1.65 Å resolution crystal structure of $NADP^+$-bound human aldose reductase (AKR1B1) was used as a model (PDB: 1ADS code). Addition of missing hydrogen atoms and computation of the protonation state of ionizable groups at pH 6.8 were carried out by using the H++ Web server (26), which relies on AMBER (27) force-field parameters and finite difference solutions to the Poisson–Boltzmann equation. The charge distribution for PGA_1-B, in which B was replaced by a methyl group, was obtained by fitting the quantum mechanically calculated (RHF 6-31G*\\3-21G*) molecular electrostatic potential to a point charge model, as implemented in Gaussian 03 (Gaussian, Inc.).

The Lamarckian genetic algorithm implemented in AutoDock 3.0.5 (28) was used to generate automated poses of PGA_1 docked within the binding site of AKR employing a dielectric constant of 2. Consistent bonded and nonbonded AMBER "gaff" parameters (parm03) were assigned to PGA_1 atoms and a molecular dynamics (MD) simulation of the selected complex in the presence of explicit water (a truncated octahedron containing 4 Na^+ ions to achieve electroneutrality) was run for 5 nanoseconds by using periodic boundary conditions. Initially, positional restraints of 5 kcal/mol on the protein α-carbons and harmonic restraints on the distances between the keto-group of PGA_1 and His111 N^{ε} and between the electrophilic carbon of PGA_1 and the sulfur atom of Cys299 were applied. After 1 nanosecond, all the restraints were removed and the solvated complex was allowed to evolve freely.

Plasmids and transfections

The plasmid pCMV6-XL5 containing human AKR1B10 ORF was from Origene. The insert was cloned into the pCEFL-KZ-AU5 plasmid to yield AU5-AKR1B10 wild type (wt). The C299S, H111A, and Y49F mutants were generated by site-directed mutagenesis by using oligonucleotides, 5′-CTGGAGGGC-CTCTAACGTGTTGCAATCCTCTCATTTGG-3′, 5′-GGACGTC-TATCTTATTGCCTGGCCACAGGGATTCAAGTCTGG-3′, and 5′-CTGTGCCTATGTCTTTCAGAATGAACATGAAGTGGG-3′, and their complementary reverse oligonucleotides, respectively. All constructions were sequenced. COS-7 cells in 6-well dishes were transfected with Lipofectamine 2000, using 2 μg of DNA per well.

AKR activity assay

Cells were lysed in 50 mmol/L sodium phosphate buffer (pH 6.8), and S100 fractions were used for AKR activity measurements. Assay mixtures contained 50 μg of protein, 10 mmol/L D,L-glyceraldehyde, and 200 μmol/L NADPH in 100 mmol/L sodium phosphate buffer (pH 6.8). After 20-minute incubation at room temperature NADPH consumption was monitored by measuring the absorbance at 340 nm in an Ultrospec 4300 pro

Published OnlineFirst April 20, 2011; DOI: 10.1158/0008-5472.CAN-10-3816

spectrophotometer (GE Biosciences). Enzymatic activity was expressed in nmol/min/mg of protein.

Doxorubicin detection

Intracellular doxorubicin was detected by confocal fluorescence microscopy on a Leica SP5 confocal microscope, using excitation and emission wavelengths of 470 and 590 nm (29). Doxorubicin fluorescence was quantitated by flow cytometry on an EPICS Coulter analyzer, using the above excitation and emission settings.

Cell migration and clonogenic assay

For wound-healing assays cells were grown to confluence and the monolayer was scratched with a 200 μL pipette tip. The width of the scratch was measured at 3 points in each well, and at various time points after treatment with the indicated agents. Relative migration was calculated as the percentage of distance migrated compared with the control well. Anchorage-independent growth was assessed as described (30). Cells were cultured for 3 weeks with 3 weekly medium replacements. Colonies were visualized by ethidium bromide staining on an UV transilluminator.

Cell-cycle analysis and detection of apoptosis

Cells treated with the various agents were detached with trypsin/EDTA and fixed with 70% ethanol in PBS. Immediately before flow cytometry analysis, cells were centrifuged and resuspended in 0.5% NP-40, 25 μg/mL propidium iodide and 25 μg/mL RNase A, and incubated in this solution for 15 minutes at room temperature. Apoptosis was detected by binding of Annexin V and propidium iodide staining, as described (31).

Statistical analysis

Experiments were carried out at least 3 times. Results are presented as average values ± SEM. Average values were compared by Student's *t* test for unpaired observations.

Results

PGA_1B selectively modifies AKR enzymes in NIH-3T3 fibroblasts

We have previously reported that biotinylated analogues of the cyPG 15d-PGJ_2 and PGA_1, selectively modify specific subsets of cellular proteins in NIH-3T3 fibroblasts (10). To identify selective targets of each cyPG we incubated cells with concentrations of 15d-PGJ_2-B or PGA_1-B resulting in a similar extent of total protein modification (10), and subsequently carried out subcellular fractionation. We detected a prominently labeled band at 37 kDa, appearing selectively in S100 fractions from PGA_1-B–treated fibroblasts (Fig. 1A). To identify this selective PGA_1-B target we employed a proteomic strategy following the enrichment of biotin-containing proteins by avidin chromatography, as schematized in Figure 1B and detailed in Supplementary Figure S1. Consistent with our previous work, initial proteomic analysis of this band identified glyceraldehyde-3-phosphate dehydrogenase (GAPDH; ref. 23). However, immunoprecipitation of GAPDH did not recover the PGA_1-B–selective target, which remained in the nonretained fraction (Supplementary Fig. S1), indicating that the presence of the abundant protein GAPDH was hampering identification of the comigrating PGA_1-B target. Consequently, combining GAPDH immunodepletion, avidin chromatography, and LC/MS-MS analysis (Fig. 1B; and Supplementary Fig. S1) allowed the identification of aldose reductase (AKR1B1) as a putative selective target for PGA_1-B (Supplementary Fig. S1). To directly evidence covalent addition of PGA_1-B to AKR enzymes we conducted 2D-electrophoresis. Samples from control, 15d-PGJ_2-B, and PGA_1-B–treated cells were resolved in duplicate gels used for transfer and detection of AKR proteins or biotin-positive spots, or for Coomassie blue staining and protein identification (Fig. 1C). Two spots were detected by the anti-AKR antibody; spot 1 showed pI and apparent molecular weight consistent with AKR1B1; MALDI-TOF MS analysis of spot 2 identified aldose reductase-related protein-2 (AKR1B8), an AKR family member expressed in murine fibroblasts. Both spots matched biotin positive spots only in the sample from PGA_1-B–treated cells (Fig. 1C, right), confirming the selectivity of their modification by PGA_1-B. Moreover, the presence of AKR enzymes in the avidin-bound fraction from PGA_1-B–treated cells, but not from control cells was confirmed by Western blot (Fig. 1D).

Molecular modeling studies of the interaction of PGA_1 with AKR enzymes

In our proposed binding mode for PGA_1 in the AKR1B1 active site, the keto-group is accepting hydrogen bonds from both the N^{ε}-protonated His111 and the hydroxyl of Tyr49 (Fig. 2A). These interactions, which remained stable during the unrestrained MD simulations, facilitate the orientation of the cyclopentenone ring in such a way that the electrophilic carbon is at a suitable distance from the sulfur atom of Cys299 (i.e., $\leq$4.0 Å) thus making it possible for the Michael reaction to proceed and yield a covalent adduct. Furthermore, in the case of the biotinylated analogue, PGA_1-B, the amide bond between PGA_1 and the spacer (Fig. 4) can establish an additional hydrogen bonding interaction with the side-chain carboxamide of Gln50 whereas the biotin moiety would be found facing the solvent. Consistent with the observed selectivity of the modification, the interactions predicted by this model could not be established in the case of the J series cyPG, 15d-PGJ_2 (data not shown).

The AKR family consists of more than 100 members, and significant homology exists among many of them (Fig. 2B). Moreover, the residues predicted by the molecular model to be involved in the interaction of PGA_1 with the enzyme are highly conserved among several members of this family. Given the high degree of sequence identity between AKR1B1 and AKR1B10, especially within the active site region (Fig. 2B), the mode of binding of PGA_1 and PGA_1-B to these 2 enzymes is expected to be identical. Given its significance in tumor biology, we used AKR1B10 for subsequent studies addressing the interactions of PGA_1 with AKR enzymes and their functional implications.

Published OnlineFirst April 20, 2011; DOI: 10.1158/0008-5472.CAN-10-3816

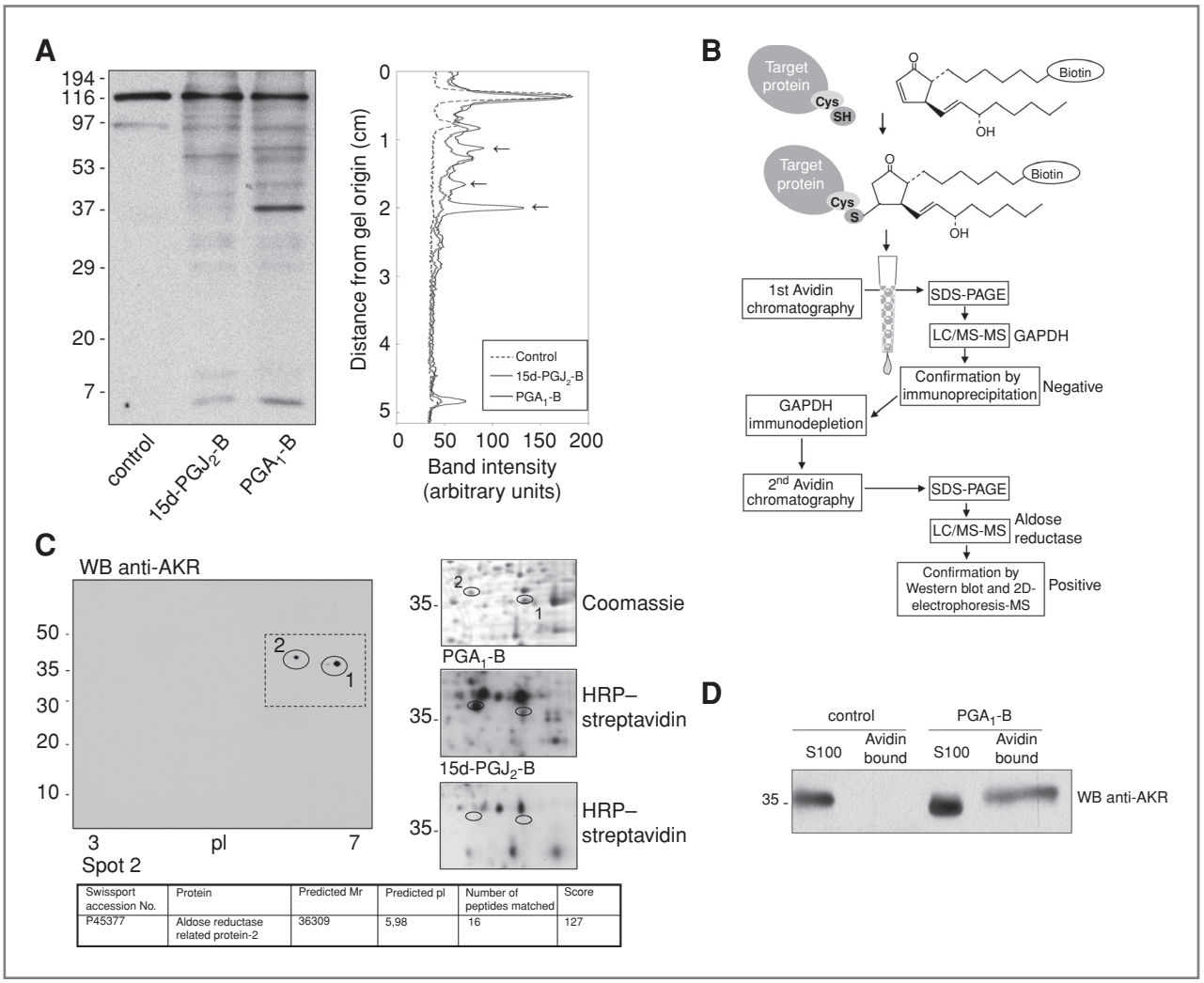

Swissport accession No.	Protein	Predicted Mr	Predicted pI	Number of peptides matched	Score
P45377	Aldose reductase related protein-2	36309	5,98	16	127

Figure 1. Identification of a protein selectively modified by PGA_1-B. A, NIH-3T3 fibroblasts were treated with vehicle [dimethylsulfoxide (DMSO), control], 5 μmol/L 15d-PGJ_2-B, or 60 μmol/L PGA_1-B, and S100 fractions were analyzed by SDS-PAGE followed by protein blotting. Biotin-containing polypeptides were detected with HRP–streptavidin (left). Band intensity was estimated by image scanning and profiles obtained for each lane are shown (right). Arrows indicate PGA_1-B selectively modified bands. B, summary of the procedure used for identification of the 37 kDa PGA_1-B selectively modified band. C, total cell lysates from NIH-3T3 fibroblasts treated with vehicle, 15d-PGJ_2-B, or PGA_1-B were separated by 2D-electrophoresis. Left, the Western blot analysis with an antibody with broad specificity to AKR family members. Right, the area of the gel in the dashed rectangle (in left) is enlarged and shown after Coomassie staining (top) or biotin detection (middle and bottom). Spots corresponding to AKR immunoreactive proteins are depicted by circles. Spot 2 was excised and subjected to tryptic digestion and MALDI-TOF MS. The identification data are summarized at the bottom. D, S100 fractions from control or PGA_1-B–treated fibroblasts were subjected to neutravidin chromatography and the retention of AKR enzymes was assessed by Western blot.

Cysteine 299 is essential for PGA_1-B binding to AKR1B10

PGA_1-B clearly formed a stable adduct with AKR1B10 in cells transiently transfected with an AU5-AKR1B10 construct, as assessed by SDS-PAGE and biotin detection (Fig. 3A). Remarkably, mutation of Cys299 to Ser virtually abolished the incorporation of PGA_1-B into AKR1B10, indicating that this residue is critical for PGA_1-B binding. Interestingly, mutation of either Tyr49 or His111 reduced the incorporation of PGA_1-B, suggesting that the presence of these residues favors the interaction of the cyPG with the active site of the enzyme as predicted by the model.

We next addressed the functional consequences of AKR1B10 modification by PGA_1. Endogenous AKR activity was negligible in COS-7 cells (see Fig. 3C). Transfection of AU5-AKR1B10 produced measurable AKR activity, which was inhibited by treatment with either PGA_1 or PGA_1-B by more than 60% (Fig. 3B), without altering AU5-AKR1B10 protein levels. In contrast, 15d-PGJ_2-B at a concentration eliciting a degree of total protein modification similar to that achieved with PGA_1-B, induced only marginal AKR1B10 labeling, and a weak inhibition of AKR activity (15%) was observed in 15d-PGJ_2–treated cells (data not shown). Remarkably, PGA_1-elicited inhibition was abolished in cells transfected with AKR1B10

Published OnlineFirst April 20, 2011; DOI: 10.1158/0008-5472.CAN-10-3816

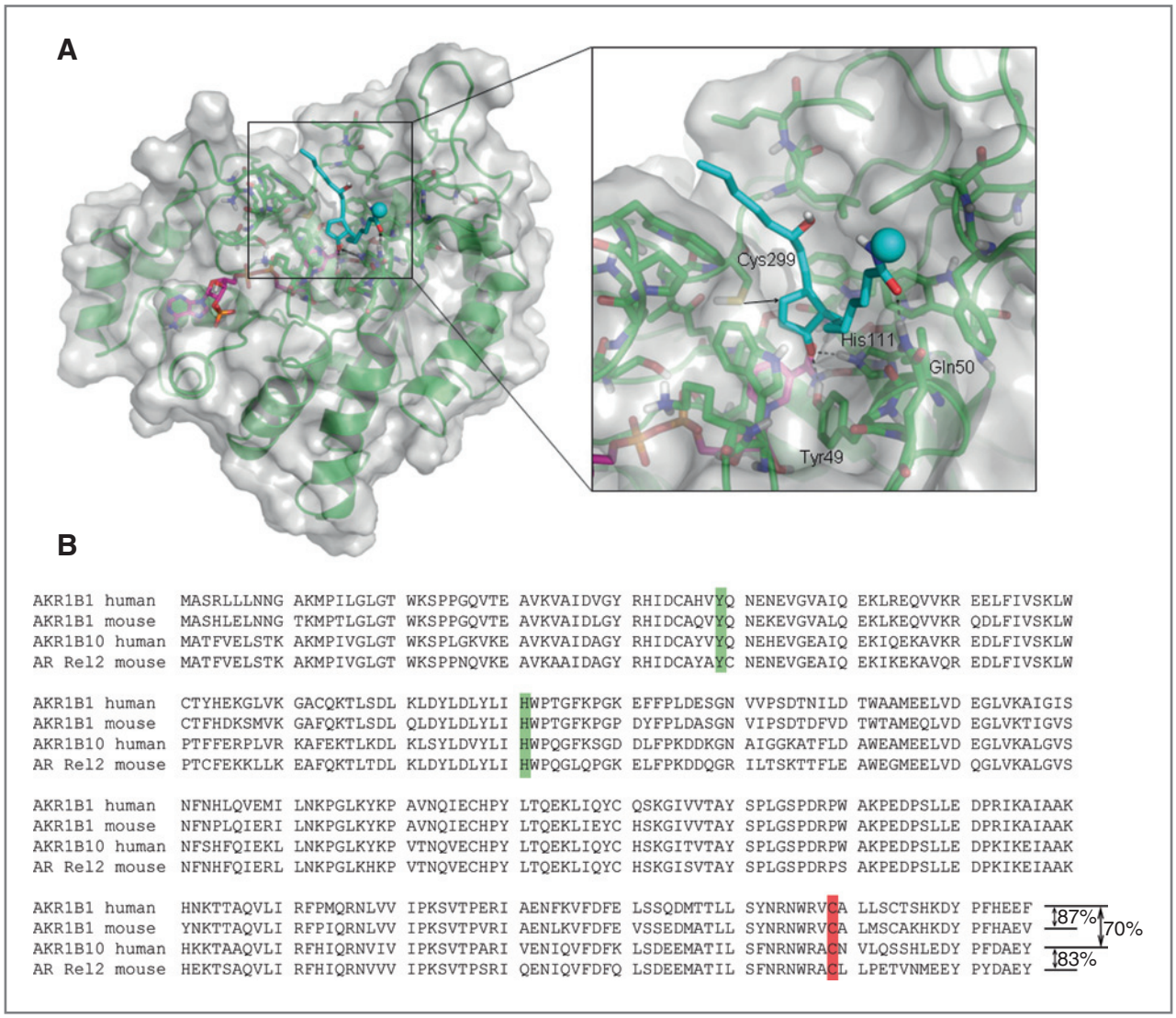

Figure 2. Proposed binding mode for PGA_1 in the aldose reductase active site. A, ribbon representation (green) of AKR1B1 with protein residues enveloped by a semitransparent solvent-accessible surface (PyMOL; DeLano Scientific, LLC). Carbon atoms of $NADP^+$ and PGA_1 are colored in magenta and cyan, respectively, and the sphere stands for the biotin moiety. The framed area on the left is enlarged in the view on the right. The protein residues most relevant to the discussion have been labeled, the hydrogen bonds involving PGA_1 are displayed as dotted lines, and the arrow points to the site of attack on the cyclopentenone ring for the sulfur atom of Cys299. B, sequences of various AKR family members. AKR1B1, aldose reductase; AR Rel-2, aldose reductase-related protein 2. The extent of identity between the various sequences is shown. Amino acids important for PGA_1 or PGA_1-B interaction with AR (AKR1B1) are shown in colored boxes. Note that amino acid numbering includes the initial methionine, which is removed in mature AKR1B1.

Cys299Ser, confirming the importance of Cys299 for both PGA_1 binding and inhibitory effect (Fig. 3C). Consistent with previous observations, the AKR1B10 Cys299Ser mutant displayed lower activity than the wt variant, reportedly due to reduced affinity for the D,L-glyceraldehyde substrate (32). Mutation of Tyr 49 or His111 abolished activity (data not shown), confirming their importance in catalysis (33).

Inhibition of AKR activity by various cyclopentenones

Given the potential biomedical interest in AKR inhibitors, we characterized PGA_1 effect in more detail. PGA_1 inhibition of AKR1B10 activity in COS-7 cells was time- and concentration-dependent (IC_{50}, 43 μmol/L; Supplementary Fig. S2). Several PGA_1-related compounds including PGA_2, 8-iso-PGA_1, and 8-iso-PGA_2 inhibited AKR1B10 activity (Fig. 4). Interestingly, the isoprostanes 8-iso-PGA_1 and 8-iso-PGA_2, isomers of the respective PG, were significantly less effective than their PG counterparts, suggesting that the *trans* orientation of the PG side chain with respect to the prostane ring is more favorable for interaction with the enzyme. Remarkably, 2-cyclopentenone did not inhibit AKR1B10, suggesting that the chains of the PG are important for docking at the active site. Of the 2 reported inhibitors of AKR enzymes, fenofibrate (34) and AD-5467 (35), only the latter showed a potent inhibitory effect. AKR and actin levels were not affected under the conditions of the assay (Fig. 4).

Published OnlineFirst April 20, 2011; DOI: 10.1158/0008-5472.CAN-10-3816

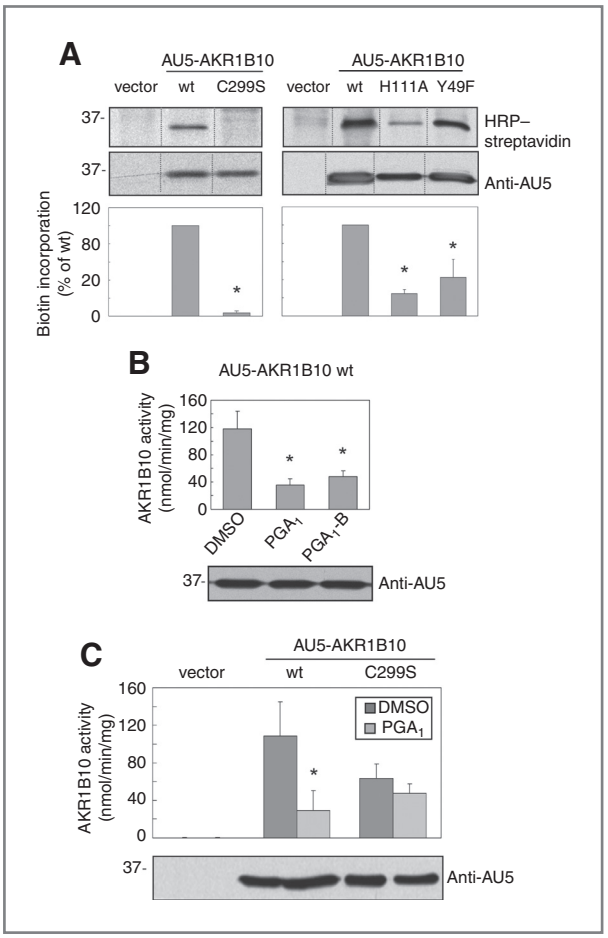

Figure 3. The interaction between PGA_1-B and AKR1B10 involves cysteine 299 and impairs enzyme activity. A, COS-7 cells transiently transfected with the indicated vectors were treated with 30 μmol/L PGA_1-B for 2 hours. Biotin incorporation was assessed as in Figure 1. Dotted lines indicate where lanes from the same gel have been cropped. Results are average values ± SEM of at least 3 experiments. *, $P < 0.05$ by Student's *t* test versus wt. B, effect of PGA_1 and PGA_1-B on AKR1B10 activity. C, PGA_1 inhibition of AKR1B10 activity requires Cys299. B and C, COS-7 cells transfected with AU5-AKR1B10 wt or Cys299Ser were treated with 60 μmol/L PGA_1, PGA_1-B, or vehicle for 24 hours, after which AKR activity was measured. Results are average values ± SEM of 5 (B) or 3 (C) experiments. *, $P < 0.05$ vs. AKR1B10 wt treated with vehicle. Levels of transfected proteins were assessed by Western blot with anti-AU5 antibody.

PGA_1 inhibits AKR activity in human lung adenocarcinoma A549 cells

In search for a biologically relevant model to assess PGA_1 effects, we explored the levels of AKR1B10 in A549, H1299, and Calu-3 lung cancer cells, of which only A549 cells showed detectable levels (Supplementary Fig. S3). PGA_1 reduced cell viability and induced cell-cycle alterations in all cells studied to variable extents (Supplementary Fig. S3). Consistent with a role of AKR1B10 in detoxification and cell survival, A549 cells showed reduced susceptibility to PGA_1 effects. Treatment of A549 cells with PGA_1-B elicited the selective retention of endogenous AKR proteins, and specifically of AKR1B10, on avidin–agarose beads (Fig. 5A), indicating that PGA_1-B modifies AKR enzymes in this cell type. Moreover, PGA_1 and PGA_1-B effectively inhibited AKR activity without altering AKR protein levels (Fig. 5B). According to previous evidence, reduced glutathione (GSH) forms stable adducts with PGA_1-type PG potentially reducing interactions with proteins (36). We previously showed that GSH depletion enhances PGA_1-B binding to cellular proteins (10). Consistent with this, treatment of A549 cells with buthionine sulfoximine (BSO), a GSH synthesis inhibitor, improved PGA_1-B incorporation into proteins and increased retention of biotin-tagged proteins onto neutravidin beads (Supplementary Fig. S4). Moreover, GSH depletion specifically increased AKR retention on avidin after PGA_1-B treatment (Fig. 5C). Furthermore, BSO showed a tendency to reduce AKR activity per se and significantly potentiated PGA_1-elicited AKR inhibition (Fig. 5D). Taken together, these results indicate that maintenance of GSH levels or of redox status is important for AKR function. In addition, GSH depletion facilitates AKR modification and inhibition by PGA_1.

Effects of PGA_1 on A549 cells tumorigenicity and drug resistance

PGA_1 inhibited A549 cell migration in a wound healing assay (Fig. 6A) and reduced anchorage-independent clonogenic growth (Fig. 6B), thus suggesting an inhibition of tumorigenic potential. AKR1B10 is involved in the metabolism of a variety of anticancer compounds, including doxorubicin and daunorubicin, potentially leading to chemoresistance (32, 37). Therefore, we explored whether PGA_1 could improve doxorubicin efficiency. The main mechanism for doxorubicin action at clinically relevant concentrations is the stabilization of a cleaved ternary topoisomerase II–doxorubicin–DNA complex, resulting in a blockade in the G_2 phase of the cell cycle (38–40). Doxorubicin treatment induced a concentration-dependent increase in the proportion of A549 cells present in the G_2–M phases of the cell cycle (Fig. 6C, left), an effect that was clearly potentiated by PGA_1 (Fig. 6C, right). This effect was associated with an improvement of doxorubicin availability in cells. PGA_1 clearly potentiated intracellular accumulation of doxorubicin at several concentrations of the drug, as assessed by flow cytometry (Fig. 6D). Confocal fluorescent microscopy confirmed PGA_1-elicited potentiation of doxorubicin retention, mainly at the nuclear compartment (Supplementary Fig. S5). The AKR inhibitor AD-5467 mimicked the effects of PGA_1 both on cell-cycle distribution and doxorubicin accumulation (data not shown). Taken together, these results suggest that PGA_1 treatment through inhibition of AKR activity in A549 cells, may increase the accumulation of the AKR substrate doxorubicin and potentiate its biological effects, helping to counteract multidrug chemoresistance.

Discussion

Proteomic studies are shedding light into the signaling and targets of endogenous electrophiles, unveiling novel mechanisms of action and providing opportunities for drug discovery (23). Our results identify AKR1B10, an enzyme involved in

Published OnlineFirst April 20, 2011; DOI: 10.1158/0008-5472.CAN-10-3816

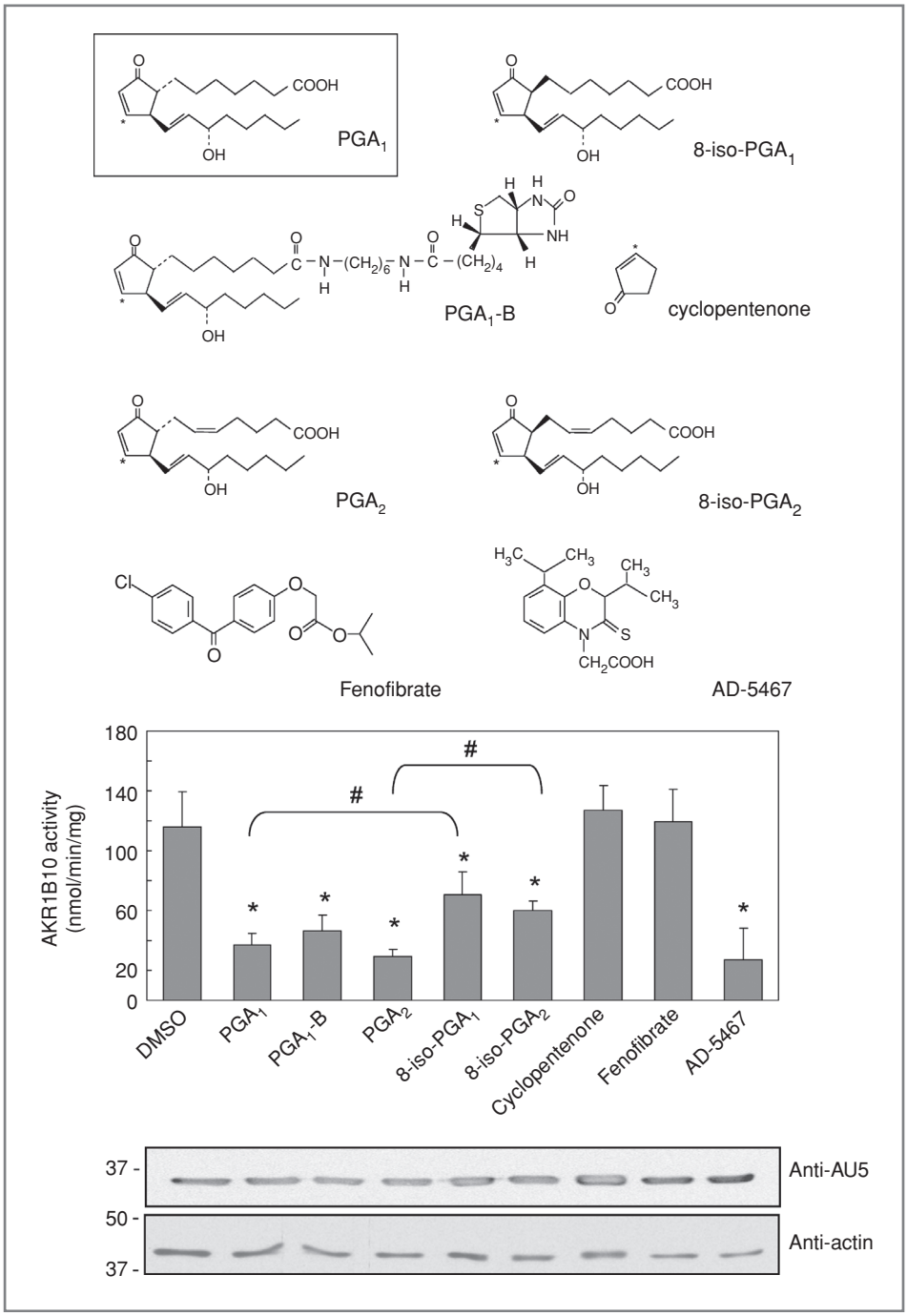

Figure 4. Effect of various cyclopentenones and reported AKR inhibitors on AKR activity. COS-7 cells transfected with AU5-AKR1B10 wt were treated with the indicated compounds at 60 μmol/L or vehicle for 24 hours before AKR activity determination. Results are average values ± SEM of 3 experiments. *, $P < 0.05$ vs. vehicle; #, $P < 0.05$ between the conditions indicated. Structures of the compounds used are shown at the top and levels of AU5-AKR1B10 and actin after the various treatments are shown at the bottom.

tumor development and cancer chemoresistance, as a selective target for modification and inhibition by A-class cyPG. Moreover, we showed that PGA_1 inhibits AKR activity in lung cancer cells, reduces their migration and anchorage-independent growth, reflecting reduced invasiveness, and potentiates the effect of the antitumoral agent doxorubicin, a known AKR1B10 substrate. Therefore, the PGA_1–AKR1B10 interaction could be explored for the development of novel strategies against tumor chemoresistance.

Insight into the structural basis for the preferential interaction of PGA_1 with AKR enzymes was obtained by molecular docking and confirmed by biochemical characterization of site-specific mutants of AKR1B10. AKR1B10, like other AKR enzymes, is a monomeric protein with an $(\alpha/\beta)_8$ barrel structure containing the active site. Residues His111, Tyr49, K79, and Asp44 line the active site, play a key role in catalysis, and are highly conserved in the AKR family (12). Cys299 is located close to the active site and modulates the interaction

Published OnlineFirst April 20, 2011; DOI: 10.1158/0008-5472.CAN-10-3816

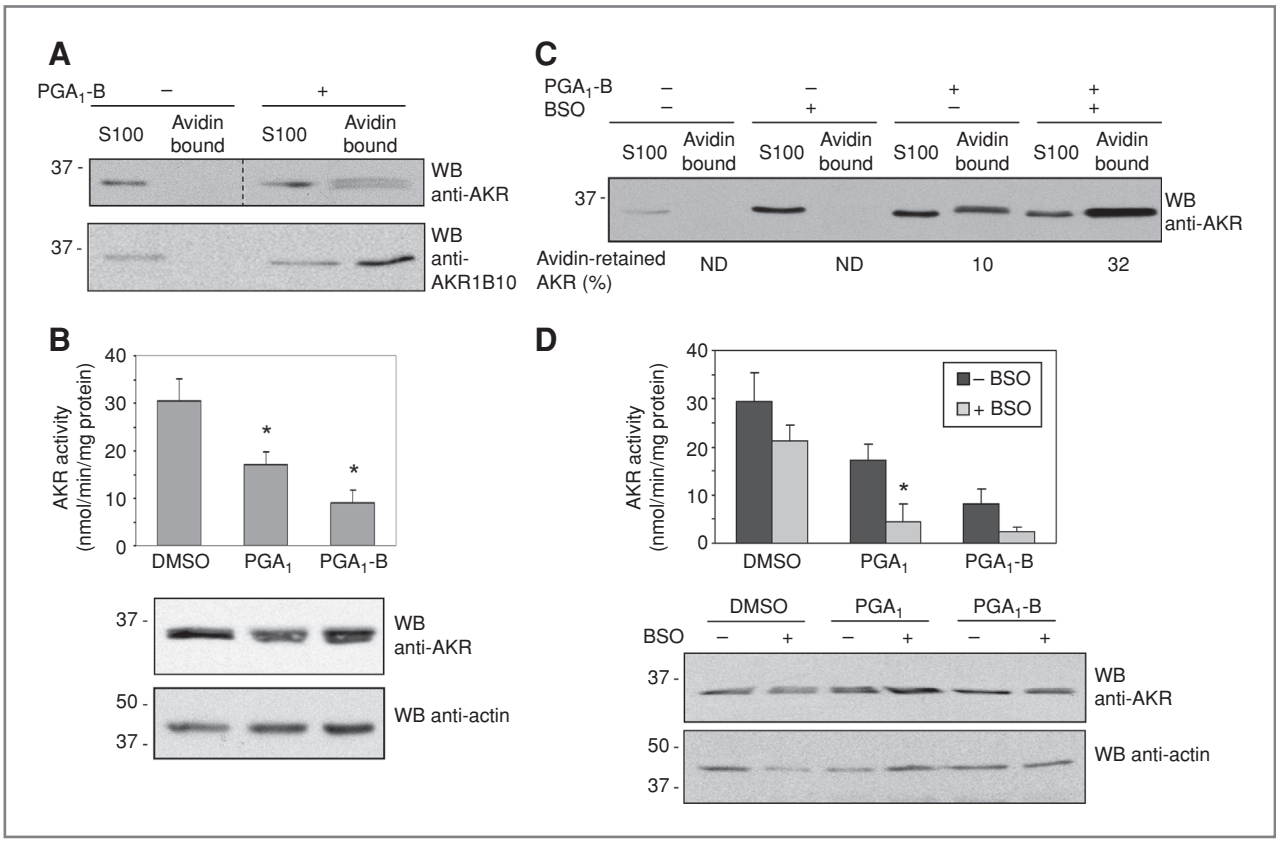

Figure 5. Modification and inhibition of AKR by PGA_1 or PGA_1-B in A549 cells. A, A549 cells were incubated with vehicle or 60 μmol/L PGA_1-B for 24 hours. S100 fractions were subjected to pull-down on avidin–agarose. The presence of AKR enzymes in the avidin-bound fraction was assessed by Western blot with anti-AKR or anti-AKR1B10 antibodies. B, A549 cells were treated with vehicle or 60 μmol/L PGA_1 or PGA_1-B for 24 hours and AKR activity was measured. Results are average values ± SEM of 5 experiments. *, $P < 0.05$ vs. vehicle by Student's *t* test. Levels of AKR and actin are shown at the bottom. C, cells were treated with vehicle or PGA_1-B as above. When indicated, cells were pretreated with 50 μmol/L BSO for 16 hours. S100 fractions were used for pull-down on avidin–agarose beads. The intensity of the protein signals was estimated by image scanning and the proportion of AKR enzymes present in the avidin-retained fractions with respect to the amount present in the starting S100 fractions are shown as average values of 4 experiments. ND, not detectable. D, A549 cells were treated with BSO followed by PGA_1 or PGA_1-B, as indicated, under the conditions specified above for determination of AKR activity. The levels of AKR and actin in S100 fractions from a representative experiment are shown at the bottom. Results are average values ± SEM of 3 experiments. *, $P < 0.05$ vs. the same condition in the absence of BSO by Student's *t* test.

of substrates and inhibitors with the enzyme. Molecular modeling studies postulated the formation of a Michael adduct between PGA_1 and AKR involving Cys299, with Tyr49 and His111 playing a facilitating role. Interestingly, mutagenesis studies confirmed the requirement for Cys299 for covalent addition of PGA_1-B to AKR1B10, whereas Tyr49 and His111 were required for optimal binding. Cys299 was also required for PGA_1-mediated inhibition of AKR1B10, confirming the functional importance of the interaction. Importantly, both PGA_1 and PGA_1-B displayed similar inhibitory effects, indicating that, in agreement with the modeling results, the biotin moiety does not interfere with the interaction. Indeed, we have confirmed modification and inhibition of recombinant AKR1B1 by both compounds (B.D-D., unpublished data).

Given the important implications of AKR1B10 in tumor development and cancer chemoresistance, the search for inhibitors of this enzyme is a thriving area of research. Several compounds have been found to display AKR1B10 inhibitory properties *in vitro*, including some nonsteroidal anti-inflammatory drugs (41), butein (42), and curcumin derivatives (43). Our results suggest that PGA-type cyPG may constitute a novel class of AKR inhibitors. PGA_1 binding to AKR1B10 shows unique characteristics among several recently identified inhibitors for this enzyme (41, 43), for which Gln114, Val301, and Gln303 or Ser304 were found to be the critical interacting residues. It would be interesting to explore whether modifications of the PGA_1 structure could be designed to increase the specificity or potency of the inhibition. Concentrations of PGA_1 used in this work should be considered pharmacologic because they are at least 3 orders of magnitude higher than those measured in biological systems (44).

A549 cells constitute a widely used cellular model of lung carcinoma and express several AKR isoforms, of which AKR1B10 is the most abundant (45). As AKR1B10 is involved in detoxification of various carbonyls, it could also confer increased resistance to PGA_1 or to reactive species generated during PGA_1 treatment. The finding that blocking GSH

Published OnlineFirst April 20, 2011; DOI: 10.1158/0008-5472.CAN-10-3816

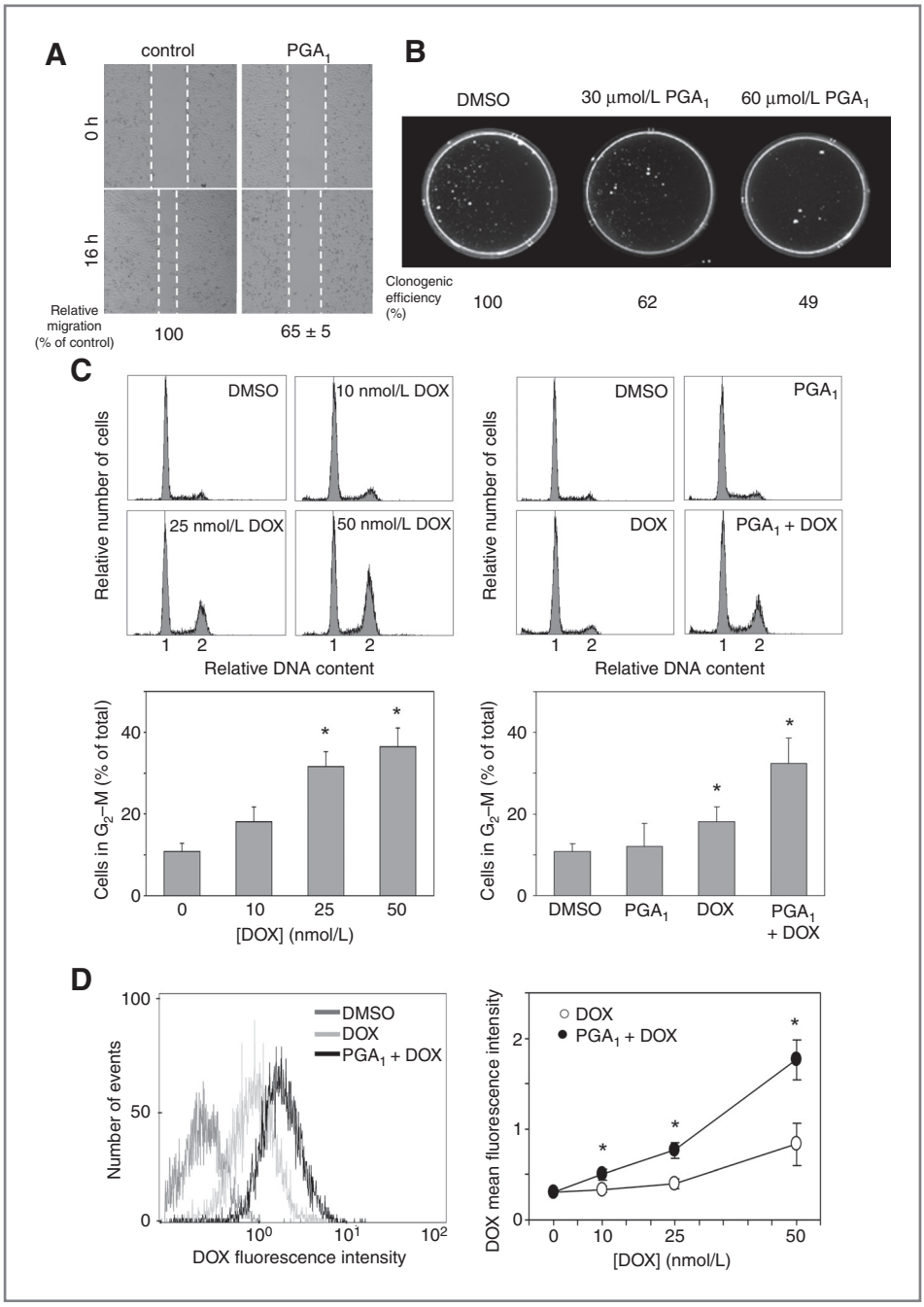

Figure 6. Effect of PGA_1 on A549 cells tumorigenicity and susceptibility to doxorubicin. Cell migration (A) and clonogenic growth (B) were assessed in A549 cells treated with vehicle or the indicated concentrations of PGA_1 in complete medium. Clonogenic efficiency was calculated as the percentage of colonies present with respect to plates treated with vehicle. C, cells were treated with the indicated concentrations of doxorubicin (DOX) for 16 hours (left) or with 10 nmol/L DOX in the absence or presence of 30 μmol/L PGA_1 for 16 hours (right). Cell-cycle distribution was analyzed by flow cytometry. Proportions of cells in the G_2–M phases shown at the bottom are average values ± SEM of 3 experiments. *, $P < 0.05$ vs. vehicle by Student's *t* test. D, determination of DOX fluorescence by flow cytometry. Left, results from a representative experiment after treatment with 50 nmol/L DOX for 16 hours in the absence or presence of 30 μmol/L PGA_1. Right, mean fluorescent intensities of cells treated with various DOX concentrations in the absence or presence of 30 μmol/L PGA_1. Results are average values ± SEM of 3 experiments (*, $P < 0.05$ vs. the same condition in the absence of PGA_1 by Student's *t* test).

synthesis improves PGA_1-elicited modification and inhibition of AKR enzymes suggests that GSH depletion could constitute a strategy to improve the antitumoral action of PGA_1-type cyPG. We have also observed that AKR inhibition in A549 cells is associated with an improvement of the effects of doxorubicin, a widely used drug in the therapy of lung (46) and other cancers (47). Doxorubicin clinical efficacy, however, is limited by the development of cancer cell resistance due to induction of drug detoxification mechanisms, including conversion by AKR enzymes to the less effective metabolite doxorubicinol (37). It should be noted that although most studies on doxorubicin action have been conducted with micromolar concentrations, the effects herein reported occur at nanomolar doxorubicin concentrations. This is closer to the levels measured in the plasma of patients receiving the drug (25–250 nmol/L) and that expected to occur *in vivo* within the tumor microenvironment (48). The fact that the AKR inhibitor AD-5467 mimics PGA_1-elicited potentiation of doxorubicin actions suggests that inhibition of AKR may be involved in PGA_1 effects. Nevertheless, because PGA_1 may bind to multiple cellular targets (23), it could exert other cellular actions contributing

Published OnlineFirst April 20, 2011; DOI: 10.1158/0008-5472.CAN-10-3816

to the improvement of doxorubicin effectiveness, including induction of reactive oxygen species, modulation of GST activity or GSH content, and interference with drug efflux. These possibilities will be the subject of further studies.

In summary, our study identifies AKR enzymes as prominent PGA_1-selective targets. Moreover, PGA_1 binds covalently and inhibits AKR1B10 establishing specific interactions with the enzyme and potentiates the effects of the antitumoral drug doxorubicin. These results unveil novel possibilities to overcome cancer chemoresistance.

Disclosure of Potential Conflicts of Interest

D. Pérez-Sala and B. Díez-Dacal are coinventors of a related patent applied for by CSIC. The other authors disclosed no potential conflicts of interest.

Grant Support

This work was supported by grants SAF2009-11642 from MiCInn and RETICS RD07/0064/0007 from ISCIII to D. Pérez-Sala and SAF2006-12713-C02-02 (CICYT) and S-BIO/0214/2006 (CAM) to F. Gago. J. Gayarre was the recipient of fellowships from CSIC (I3P), EMBO, and FEBS (short term fellowships). C. Coderch was supported by a MiCInn FPU (AP2007-01225) fellowship. Part of this work was undertaken at UCLH/UCL who received a proportion of funding from the Department of Health's NIHR Biomedical Research Centres funding scheme. Feedback from COST Action CM1001 is appreciated.

The costs of publication of this article were defrayed in part by the payment of page charges. This article must therefore be hereby marked *advertisement* in accordance with 18 U.S.C. Section 1734 solely to indicate this fact.

Received October 19, 2010; revised March 29, 2011; accepted April 11, 2011; published OnlineFirst April 20, 2011.

References

1. Cernuda-Morollón E, Pineda-Molina E, Cañada FJ, Pérez-Sala D. 15-Deoxy-$\Delta^{12,14}$-prostaglandin J_2 inhibition of NF-κB DNA binding through covalent modification of the p50 subunit. J Biol Chem 2001;276:35530–6.
2. Levonen AL, Dickinson DA, Moellering DR, Mulcahy RT, Forman HJ, Darley-Usmar VM. Biphasic effects of 15-deoxy-delta(12,14)-prostaglandin J(2) on glutathione induction and apoptosis in human endothelial cells. Arterioscler Thromb Vasc Biol 2001;21:1846–51.
3. Díez-Dacal B, Pérez-Sala D. Anti-inflammatory prostanoids: focus on the interactions between electrophile signalling and resolution of inflammation. ScientificWorldJournal 2010;10:655–75.
4. Sánchez-Gómez FJ, Cernuda-Morollón E, Stamatakis K, Pérez-Sala D. Protein thiol modification by 15-deoxy-$\Delta^{12,14}$-prostaglandin J_2 addition in mesangial cells: role in the inhibition of pro-inflammatory genes. Mol Pharmacol 2004;66:1349–58.
5. Shiraki T, Kamiya N, Shiki S, Kodama TS, Kakizuka A, Jingami H. α,ß-unsaturated ketone is a core moiety of natural ligands for covalent binding to peroxisome proliferator-activated receptor. J Biol Chem 2005;280:14145–53.
6. Pérez-Sala D, Cernuda-Morollón E, Cañada FJ. Molecular basis for the inhibition of AP-1 DNA binding by 15-deoxy-$\Delta^{12,14}$-prostaglandin J_2. J Biol Chem 2003;278:51251–60.
7. Rossi A, Kapahi P, Natoli G, Takahashi T, Chen Y, Karin M, et al. Anti-inflammatory cyclopentenone prostaglandins are direct inhibitors of IκB kinase. Nature 2000;403:103–8.
8. Straus DS, Pascual G, Li M, Welch JS, Ricote M, Hsiang CH, et al. 15-deoxy-delta(12,14)-prostaglandin J2 inhibits multiple steps in the NF-kappaB signaling pathway. Proc Natl Acad Sci U S A 2000;97:4844–9.
9. Renedo M, Gayarre J, García-Domínguez CA, Pérez-Rodríguez A, Prieto A, Cañada FJ, et al. Modification and activation of Ras proteins by electrophilic prostanoids with different structure are site-selective. Biochemistry 2007;46:6607–16.
10. Gayarre J, Stamatakis K, Renedo M, Pérez-Sala D. Differential selectivity of protein modification by the cyclopentenone prostaglandins PGA_1 and 15-deoxy-$\Delta^{12,14}$-PGJ_2: role of glutathione. FEBS Lett 2005;579:5803–8.
11. Doyle K, Fitzpatrick FA. Redox signaling, alkylation (carbonylation) of conserved cysteines inactivates class I histone deacetylases 1, 2, and 3 and antagonizes their transcriptional repressor function. J Biol Chem 2010;285:17417–24.
12. Petrash JM. All in the family: aldose reductase and closely related aldo-keto reductases. Cell Mol Life Sci 2004;61:737–49.
13. Cao D, Fan ST, Chung SS. Identification and characterization of a novel human aldose reductase-like gene. J Biol Chem 1998;273:11429–35.
14. Fukumoto S, Yamauchi N, Moriguchi H, Hippo Y, Watanabe A, Shibahara J, et al. Overexpression of the aldo-keto reductase family protein AKR1B10 is highly correlated with smokers' non-small cell lung carcinomas. Clin Cancer Res 2005;11:1776–85.
15. Kim B, Lee HJ, Choi HY, Shin Y, Nam S, Seo G, et al. Clinical validity of the lung cancer biomarkers identified by bioinformatics analysis of public expression data. Cancer Res 2007;67:7431–8.
16. Satow R, Shitashige M, Kanai Y, Takeshita F, Ojima H, Jigami T, et al. Combined functional genome survey of therapeutic targets for hepatocellular carcinoma. Clin Cancer Res 2010;16:2518–28.
17. Li CP, Goto A, Watanabe A, Murata K, Ota S, Niki T, et al. AKR1B10 in usual interstitial pneumonia: expression in squamous metaplasia in association with smoking and lung cancer. Pathol Res Pract 2008;204:295–304.
18. Gallego O, Ruiz FX, Ardevol A, Dominguez M, Alvarez R, de Lera AR, et al. Structural basis for the high all-trans-retinaldehyde reductase activity of the tumor marker AKR1B10. Proc Natl Acad Sci U S A 2007;104:20764–9.
19. Ruiz FX, Gallego O, Ardevol A, Moro A, Dominguez M, Alvarez S, et al. Aldo-keto reductases from the AKR1B subfamily: retinoid specificity and control of cellular retinoic acid levels. Chem Biol Interact 2009;178:171–7.
20. Martin HJ, Breyer-Pfaff U, Wsol V, Venz S, Block S, Maser E. Purification and characterization of AKR1B10 from human liver: role in carbonyl reduction of xenobiotics. Drug Metab Dispos 2006;34:464–70.
21. Hausding M, Witteck A, Rodríguez-Pascual F, von Eichel-Streiber C, Fostermann U, Kleinert H. Inhibition of small G proteins of the Rho family by statins or clostridium difficile toxin B enhances cytokine-mediated induction of NO synthase II. Br J Pharmacol 2000;131:553–61.
22. Edgell CJ, McDonald CC, Graham JB. Permanent cell line expressing human factor VIII-related antigen established by hybridization. Proc Natl Acad Sci USA 1983;80:3734–7.
23. Garzón B, Gayarre J, Gharbi S, Díez-Dacal B, Sánchez-Gómez FJ, Timms JF, et al. A biotinylated analog of the anti-proliferative prostaglandin A_1 allows assessment of PPAR-independent effects and identification of novel cellular targets for covalent modification. Chem Biol Interact 2010;183:212–21.
24. George R, Chan HL, Ahmed Z, Suen KM, Stevens CN, Levitt JA, et al. A complex of Shc and Ran-GTPase localises to the cell nucleus. Cell Mol Life Sci 2009;66:711–20.
25. Gharbi S, Gaffney P, Yang A, Zvelebil MJ, Cramer R, Waterfield MD, et al. Evaluation of two-dimensional differential gel electrophoresis for proteomic expression analysis of a model breast cancer cell system. Mol Cell Proteomics 2002;1:91–8.
26. Gordon JC, Myers JB, Folta T, Shoja V, Heath LS, Onufriev A. H++: a server for estimating pKas and adding missing hydrogens to macromolecules. Nucleic Acids Res 2005;33:W368–71.
27. Cornell W, Cieplak P, Bayly C, Gould I, Merz K, Ferguson D, et al. A second generation force field for the simulation of proteins, nucleic acids and organic molecules. J Am Chem Soc 1995;117:5179–97.
28. Morris G, Goodsell D, Halliday R, Huey R, Hart W, Belew R, et al. Automated docking using a Lamarckian genetic algorithm and an

Published OnlineFirst April 20, 2011; DOI: 10.1158/0008-5472.CAN-10-3816

empirical binding free energy function. J Comput Chem 1998;19:1639–62.
29. Aroui S, Brahim S, Waard MD, Kenani A. Cytotoxicity, intracellular distribution and uptake of doxorubicin and doxorubicin coupled to cell-penetrating peptides in different cell lines: a comparative study. Biochem Biophys Res Commun 2010;391:419–25.
30. Ogretmen B, Schady D, Usta J, Wood R, Kraveka JM, Luberto C, et al. Role of ceramide in mediating the inhibition of telomerase activity in A549 human lung adenocarcinoma cells. J Biol Chem 2001;276:24901–10.
31. Sánchez-Gómez FJ, Díez-Dacal B, Pajares MA, Llorca O, Pérez-Sala D. Cyclopentenone prostaglandins with dienone structure promote cross-linking of the chemoresistance-inducing enzyme glutathione transferase P1-1. Mol Pharmacol 2010;78:723–33.
32. Balendiran GK, Martin HJ, El-Hawari Y, Maser E. Cancer biomarker AKR1B10 and carbonyl metabolism. Chem Biol Interact 2009;178:134–7.
33. Bohren KM, Grimshaw CE, Lai CJ, Harrison DH, Ringe D, Petsko GA, et al. Tyrosine-48 is the proton donor and histidine-110 directs substrate stereochemical selectivity in the reduction reaction of human aldose reductase: enzyme kinetics and crystal structure of the Y48H mutant enzyme. Biochemistry 1994;33:2021–32.
34. Verma M, Martin HJ, Haq W, O'Connor TR, Maser E, Balendiran GK. Inhibiting wild-type and C299S mutant AKR1B10; a homologue of aldose reductase upregulated in cancers. Eur J Pharmacol 2008;584:213–21.
35. Ohtori A, Yamamoto Y, Tojo KJ. Penetration and binding of aldose-reductase inhibitors in the lens. Invest Ophthalmol Vis Sci 1991;32:189–93.
36. Suzuki M, Mori M, Niwa T, Hirata R, Furuta K, Ishikawa T, et al. Chemical implications for antitumor and antiviral prostaglandins: reaction of Δ^7-prostaglandin A_1 and prostaglandin A_1 methyl esters with thiols. J Am Chem Soc 1997;119:2376–85.
37. Veitch ZW, Guo B, Hembruff SL, Bewick AJ, Heibein AD, Eng J, et al. Induction of 1C aldoketoreductases and other drug dose-dependent genes upon acquisition of anthracycline resistance. Pharmacogenet Genomics 2009;19:477–88.
38. Stravopodis DJ, Karkoulis PK, Konstantakou EG, Melachroinou S, Lampidonis AD, Anastasiou D, et al. Grade-dependent effects on cell cycle progression and apoptosis in response to doxorubicin in human bladder cancer cell lines. Int J Oncol 2009;34:137–60.
39. Dan S, Yamori T. Repression of cyclin B1 expression after treatment with adriamycin, but not cisplatin in human lung cancer A549 cells. Biochem Biophys Res Commun 2001;280:861–7.
40. Goto S, Ihara Y, Urata Y, Izumi S, Abe K, Koji T, et al. Doxorubicin-induced DNA intercalation and scavenging by nuclear glutathione S-transferase pi. FASEB J 2001;15:2702–14.
41. Endo S, Matsunaga T, Soda M, Tajima K, Zhao HT, El-Kabbani O, et al. Selective inhibition of the tumor marker AKR1B10 by antiinflammatory n-phenylanthranilic acids and glycyrrhetic acid. Biol Pharm Bull 2010;33:886–90.
42. Song DG, Lee JY, Lee EH, Jung SH, Nho CW, Cha KH, et al. Inhibitory effects of polyphenols isolated from Rhus verniciflua on aldo-keto reductase family 1 B10. BMB Rep 2010;43:268–72.
43. Matsunaga T, Endo S, Soda M, Zhao HT, El-Kabbani O, Tajima K, et al. Potent and selective inhibition of the tumor marker AKR1B10 by bisdemethoxycurcumin: probing the active site of the enzyme with molecular modeling and site-directed mutagenesis. Biochem Biophys Res Commun 2009;389:128–32.
44. Garzón B, Oeste CL, Díez-Dacal B, Pérez-Sala D. Proteomic studies on protein modification by cyclopentenone prostaglandins: expanding our view on electrophile actions. J Proteomics 2011. [Epub ahead of print].
45. Quinn AM, Harvey RG, Penning TM. Oxidation of PAH trans-dihydrodiols by human aldo-keto reductase AKR1B10. Chem Res Toxicol 2008;21:2207–15.
46. Oze I, Hotta K, Kiura K, Ochi N, Takigawa N, Fujiwara Y, et al. Twenty-seven years of phase III trials for patients with extensive disease small-cell lung cancer: disappointing results. PLoS One 2009;4:e7835.
47. Hurley LH. DNA and its associated processes as targets for cancer therapy. Nat Rev Cancer 2002;2:188–200.
48. Minotti G, Menna P, Salvatorelli E, Cairo G, Gianni L. Anthracyclines: molecular advances and pharmacologic developments in antitumor activity and cardiotoxicity. Pharmacol Rev 2004;56:185–229.

Cancer Research
The Journal of Cancer Research (1916–1930) | The American Journal of Cancer (1931–1940)

AACR American Association for Cancer Research

Identification of Aldo-Keto Reductase AKR1B10 as a Selective Target for Modification and Inhibition by Prostaglandin A_1: Implications for Antitumoral Activity

Beatriz Díez-Dacal, Javier Gayarre, Severine Gharbi, et al.

Cancer Res 2011;71:4161-4171. Published OnlineFirst April 20, 2011.